Published in final edited form as:
Integr Biol (Camb). 2009 February ; 1(2): 212–219. doi:10.1039/b818874b.

Mechanical and spatial determinants of cytoskeletal geodesic dome formation in cardiac fibroblasts

Emilia Entcheva and **Harold Bien**
Department of Biomedical Engineering, Stony Brook University, HSC T18-030, Stony Brook, NY 11794-8181, USA., Tel: +1 631-444-2368

Emilia Entcheva: emilia.entcheva@sunysb.edu

Abstract

This study tests the hypothesis that the cell cytoskeletal (CSK) network can rearrange from geodesic dome type structures to stress fibers in response to microenvironmental cues. The CSK geodesic domes are highly organized actin microarchitectures within the cell, consisting of ordered polygonal elements. We studied primary neonatal rat cardiac fibroblasts. The cues used to trigger the interconversion between the two CSK architectures (geodesic domes and stress fibers) included factors affecting spatial order and the degree of CSK tension in the cells. Microfabricated three-dimensional substrates with micrometre sized grooves and peaks were used to alter the spatial order of cell growth in culture. CSK tension was modified by 2,3-butanedione 2-monoxime (BDM), cytochalasin D and the hyphae of *Candida albicans*. CSK geodesic domes occurred spontaneously in about 20% of the neonatal rat cardiac fibroblasts used in this study. Microfabricated structured surfaces produced anisotropy in the cell CSK and effectively converted geodesic domes into stress fibers in a dose-dependent manner (dependence on the period of the features). Affectors of actin structure, inhibitors of CSK tension and cell motility, *e.g.* BDM, cytochalasin D and the hyphae of *C. albicans*, suppressed or eliminated the geodesic domes. Our data suggest that the geodesic domes, similar to actin stress fibers, require maintenance of CSK integrity and tension. However, microenvironments that promote structural anisotropy in tensed cells cause the transformation of the geodesic domes into stress fibers, consistent with topographic cell guidance and some previous CSK model predictions.

Introduction

The cell cytoskeleton provides the basis for transducing mechanical signals into biochemical signals and regulating cell function. The cytoskeleton is considered an adaptable structure with ability to maintain continuous tension while rearranging itself geometrically in response to dynamic microenvironments. Hence a naturally isotropic CSK spherical form can theoretically convert to a linear bundle arrangement if anisotropic cues are provided. In anchorage-dependent cells these two forms correspond to two distinct CSK arrangements: the more common actin stress fiber formation and the “geodesic dome”, “geodome” or “polygonal net” formation. The latter CSK form is much less studied experimentally[1–4] but

Correspondence to: Emilia Entcheva, emilia.entcheva@sunysb.edu.

has been an integral part of recent computational models of the cytoskeleton of adherent[5] and non-adherent cells.[6,7] It represents a highly organized microarchitecture within the cell, consisting of ordered polygonal (triangular) elements, which typically show in F-actin staining. The two CSK forms are believed to differ in their interaction with the extracellular matrix (ECM) and their association with the underlying focal adhesions. The geodesic domes are viewed as the CSK of retracted cells with reduced adhesion to the substrate,[8] hence assuming a more spherical shape to minimize elastic energy as seen in a typical prestressed structure.[5,9]

Previous reports indicate as high as 30 to 40% occurrence of geodesic domes in rat embryonic fibroblasts and a smaller percentage in a couple of other cell types (epitheloid rabbit cell line, human dermal fibroblasts, BALB mouse cell line) shortly after trypsinization and plating, before cells fully settle and adhere.[1,3,10–12] Consequently, the geodomes have been described as developmental transient structures, precursors of stress fibers,[10] with their struts forming the sarcomere basis in muscle cells.[4] Their molecular composition has been elucidated by Lazarides and others:[10,12] the struts of the polygonal nets stain for actin and tropomyosin, the vertices for actin and α-actinin. Their exact role and importance are unknown. In most of the cases, the presumption has been made that the geodome type of CSK is only a transitional structure that inevitably evolves into a stress fiber type of arrangement, thus none of these earlier studies has tested if the presence of geodomes persists well beyond the initial re-plating phase. Also, no previous study has attempted to actively modulate the occurrence of these CSK configurations.

In this report we explore the modulating factors in the interconversion between two types of discrete CSK architectures: geodesic domes and stress fibers. We hypothesize that the geodesic domes are not simply an immediate post-trypsin artifact, but rather a dynamic alternative to the stress fiber CSK conformation that could be controlled. More specifically, we quantify the CSK reorganization in response to two modulating factors: (1) cellular spatial order, as dictated by the structure and topography of the underlying surface, and (2) cytoskeletal integrity and tension. The study of structural alterations guided by cardiac fibroblasts can potentially offer a better understanding of the interaction of a cell with its environment and the ensuing functional changes in the heart.

Results and discussion

Occurrence and characteristics of CSK geodesic domes

Geodesic dome structures, or polygonal actin nets, occupying most of the cell CSK, were found in approximately 20% of all primary cardiac fibroblasts examined well beyond the initial re-plating hours. We observed long-term preservation of the relative proportion of geodomes in our cultures up to two weeks after plating, even though the bulk of the experiments were conducted within the first week after plating. The percentage was similar for cells plated to confluency on control polydimethylsiloxane (PDMS) scaffolds and polyvinylchloride (PVC) surfaces, but was slightly lower (not statistically significant) for cells grown on glass (mean ± s.e.m.: n=7 PDMS 20 ± 3%, n = 4 PVC 19 ± 6% and n = 9 glass 16 ± 2%, n is the number of scaffolds examined). The rigidity of the scaffolds might be linked to the probability of geodome occurrence, although the softest, PDMS surfaces

employed here (with the highest percentage of geodomes), had elastic modulus 1–2 MPa (determined by uniaxial tensile testing)—at least an order of magnitude higher than the values reported for fibroblast cytoplasm. Our attempts to plate the fibroblasts at extremely low cell density (5 k cm^{-2}) did not produce geodomes. A certain threshold cell density might be necessary to stimulate cells' CSK reorganization. In this study we operated in supra-threshold cell densities (>20 k cm^{-2}), at which no correlation was found between further change in cell density and geodome frequency ($r^2 = 0.015$).

Confocal fluorescence imaging revealed amore 3D appearance for the CSK of the geodesic domes, typically wrapped around the cell nucleus. In contrast, the alternative stress-fiber form of F-actin was confined to the basal cell regions close to the scaffold surface, with the nucleus often sitting on top of the CSK (Fig. 1).

In a 2D cross-section, the geodesic dome types of cell appeared smaller and had correspondingly smaller and rounder nuclei (Fig. 2). Statistically significant reductions in size and aspect ratio (major-to-minor axis) were found for the nuclei of the geodomes *vs.* stress-fiber types of cell ($n = 11$ scaffolds for both groups, $p < 0.005$). The average area of the nucleus was significantly different in the two groups, 1000 ± 56 and 689 ± 51 μm^2, and the aspect ratio also differed, 1.49 ± 0.04 and 1.16 ± 0.04. These results are consistent with the notion of the geodomes as retracted, naturally isotropic structures, with minimum external tensile forces acting on the CSK and the nuclear lattice.[8,13]

Whole geodesic domes (polygonal nets covering an entire cell), quantified here, often exhibited higher net density in the cell periphery and the perinuclear regions (Fig. 3A). This might be partially due to the projection of 3D structures with a steep height gradient onto a 2D image. The average strut dimension (the distance between 2 vertices) for polygonal nets covering a whole cell was 3.2 ± 0.1 μm, ranging from 1.6 to 5.7 μm ($n = 160$ struts). Our estimate is close to previously reported dimensions of 3.8 μm in primary rat embryonic cells,[10] 4–5 μm in epitheloid rabbit cell line[12] and 3.5 μm in chick embryonic cells.[4] Partial polygonal nets, covering a small portion of the cell, seemed to be associated with the cells' peripheral regions or the leading edge (arrows in Fig. 3A, B). Filopodia extend from the vertices of the geodesic domes, as shown also in ref. 10.

Complex effects of topography on the CSK geodesic domes

Surface topography has been recognized as a potent cell shape modulator and an important factor in CSK organization.[14–16] In the topographic guidance theory by Curtis and Clark the cytoskeleton reorganization plays a central role in the cellular responses to surface features. Our experimental design (Fig. 4) involved three-dimensional microscale landscapes, similar to ref. 16 and 17, as opposed to 2D micropatterned geometrically constrained islands of ECM.[18] Our reasoning was that such a model might produce a more "natural" setting for cell self-organization in response to topography and structural anisotropy, avoiding ECM–non-ECM boundary effects. Indeed, previous results from our lab with cardiomyocytes grown on microfabricated surfaces demonstrated the induction of significant functional changes.[19,20]

The cells grew, following the 3D landscape (not confined to the valleys or plateaus), yet the surface features did change the cell network arrangement. Using fluorescence microscopy (inherently a 2D technique), we analyzed the cells growing on the b-portion of the surfaces (Fig. 4). Increasing the level of structure and enforced anisotropy (from case 1 to 4), led to a significant reduction in the frequency of occurrence of the geodesic domes (percentage dropped from 20% to about 6% for the highly anisotropic surfaces of cases 3 and 4), while no clear trend was observed in the corresponding cell density as a function of surface features. The percentage of observed geodomes correlated well with the period of the surface features (a + b in Fig. 4) on grooved scaffolds ($r^2 = 0.93$ for linear regression), but not on peak-surfaces.

The modulation of geodome frequency was not likely linked to increase in surface area (a potential interfering factor in 3D surfaces), because: (1) the area increase for grooves and peaks with respect to flat surfaces was the same, yet the effect on geodomes was different; and (2) the area increase for cases 1–4 was non-monotonic (9.5%, 11.8%, 11.1% and 9.5%, respectively), in contrast to the geodome frequency trends. Similarly, no clear trend of topography effects on estimated cell density was observed, thus change in cell density was not responsible for geodome modulation. We summarize, that *more structured, anisotropic environments promote the conversion of geodesic domes into stress-fiber types of CSK architecture*. These observations corroborate distinct geometry-sensing abilities of the cytoskeleton and its response *via* discrete restructuring, in line with the topographic guidance theory,[14,15] where scaffold structure leads to ECM reorganization and subsequent CSK reorganization towards a more aligned (stress fiber) appearance. Previous CSK models of erythrocytes or other cells/tissues yielded similar results when modeling cells under anisotropic loads.[7,21]

Potential geodesic domes' links to cytoskeleton integrity and prestress

A second central aim of this study was to probe the connection between CSK integrity and tension and the frequency of occurrence of the geodesic domes. The interventions used in this study to alter the cell CSK (BDM, cytochalasin D and *C. albicans*) are known to reduce CSK tension,[22] reduce the CSK elastic modulus[23–26] and reduce cell motility[23,27,28] through differing mechanisms.

In BDM-treated fibroblasts ($n = 10$ scaffolds), the number of geodesic domes dramatically decreased, regardless of surface material: 3 ± 1% for BDM-treated *vs.* 18 ± 2% for control, including PDMS, PVC and glass (Fig. 5), $p < 0.00001$. At the same time, BDM treatment for 24 h had no effect on cell density. Treated cells appeared well packed with clearly defined boundaries, partially preserved stress fibers, altered lamellipodium and no filopodia (Fig. 6A).

BDM disrupts the actomyosin contractile apparatus of the cell, which is believed to be responsible for the active generation of CSK tension.[29] In our experiments, BDM also clearly eliminated filopodia extensions (Fig. 6), consistent with previous reports on BDM as a motility inhibitor.[27] The modulating effects of BDM on the existence of the geodomes were substantial (Fig. 5B), considering that the actin network is not being destroyed by BDM and perhaps the main alteration was a change in the state of CSK tension *via*

disruption of the actin–myosin machinery. However, caution should be exerted in interpreting our results as exclusively dependent on BDM-altered CSK tension—recently multiple other effects were found for BDM treatment of cells, including regulation of the actin structure by inhibition of actin incorporation at the leading edge.[30]

The second modulating agent used, cytochalasin D, acts more directly on the actin network. Its action *in vivo*[31] involves potent disruption of the actin network organization, extensive arborization and formation of F-actin foci associated with connections to the ECM, as seen also in our experiments (Fig. 6B). Schliwa proposed that the network disruption happens mainly through removal of small network elements or through inhibition of annealing of spontaneously breaking filaments, rather than through depolymerization. This idea was supported by findings of short F-actin filaments released in the supernatant, 0.5–4 μm in size, remarkably close to the strut size in the geodomes found in this study (1.6 to 5.7 μm).

Cytochalasin D treatment for 3 h at 1 μM, on the other hand, resulted in more dramatic disturbances in the CSK: partial disintegration of the stress fibers with bright spot appearance, most likely associated with the focal adhesion sites of actin to the ECM (Fig. 6B). Geodesic domes were completely eliminated by cytochalasin D (n = 10 scaffolds). To examine if the effect is dose-dependent, we applied a 5 times lower concentration: 0.2 μM (n = 5 scaffolds). As soon as 45 min after the treatment, the geodomes were completely eliminated despite the very subtle distortion of the CSK stress fibers compared to the 1 μM treatment.

Through the interference with the integrity of the actin lattice—a major stress-bearing component of the CSK, responsible for tension maintenance—the geodomes were eliminated. Unlike the stress fibers, which seemed preserved at low concentrations, the geodomes showed exquisite sensitivity to cytochalasin D. Previous study[23] found that cells can respond to concentrations of cytochalasin D as low as 2 nM with changes in stiffness. A concentration of 0.25 μM was reported as the half-maximal dose in terms of the resultant reduction in stiffness and generated force compared to non-treated cells. These findings of extreme sensitivity of the cell mechanical state to cytochalasin D and the wide range of action (2 nM–2 μM) are consistent with our observations on the essential role of CSK prestress (and its cytochalasin D modulation) on the occurrence of the geodome structures. It has to be noted that, in addition to effects on CSK stiffness, cytochalasin D may also simply cleave/act first on the more exposed geodomes rather than the better cross-linked actin stress fibers.

Finally, we used *C. albicans* as a tool for examining *local* effects on the cytoskeleton. *C. albicans* has been reported to secrete actin-rearranging factor, reducing the proportion of filamentous actin.[24,28] The yeast treatment of the fibroblasts provided us with a convenient tool to examine the immediate local effects of fungal hyphae on the geodomes existence. Treatment with *C. albicans* for 9 h (n = 10 scaffolds) showed negligible (Fig. 7B) to significant (Fig. 7D) disturbance of the actin CSK underneath the fully developed yeast hyphae (Fig. 7A, C). The number of geodesic domes was greatly reduced, and in the high-density yeast-treated cultures practically eliminated. More specifically, a local inverse relationship was observed: no hyphae could be seen co-localized with the few remaining

geodomes (Fig. 8A, C), and, conversely, no geodomes were present under the hyphae (Fig. 8B), which unequivocally linked the geodome existence to the state of the actin microfilaments. Yeast treatment did not affect cell viability. Our use of mutant *C. albicans* prevented typical contamination processes, however, it does not preclude multiple other effects on the cells.

The results obtained with the three pharmacological treatments above support the idea that *intact actin lattice and preserved CSK tension are essential in maintaining highly organized structures like the geodesic domes*, in line with previous experimental results on actin CSK-dictated deformability in other adherent (endothelial) cells.[29,32] But our study has a couple of limitations. For definitive links of geodome existence to CSK tension, direct measurements of the latter should be employed in future studies. Furthermore, all perturbations applied in this study resulted in inhibition of CSK geodomes; in future experiments it would be informative to test stimulants of CSK prestress, *e.g.* histamine or angiotensin II, and hence potential promoters of geodomes. Another limitation of this study is that it could not resolve whether the geodomes represent a dynamic CSK conformation typical for all cells, or alternatively a distinct population of cells adopts such architecture under the proper circumstances, thus the term “interconversion” used here should be taken with caution. Real-time fluorescence microscopy might be useful in tracking the evolution of the geodomes with time. However, such labeling and *long-term* imaging of fine actin structures (<4 μm) in *live* cells without artifacts and fuzziness are extremely challenging. An alternative is perhaps a non-fluorescent approach using differential interference contrast microscopy for continuous monitoring.

Broader implications

The geodesic domes, examined in this study, are distinct highly organized CSK microarchitectures, which are dynamically controlled by external and internal forces. Their existence in a large variety of cell types points to a universal CSK property. It is interesting to note that they are most often seen in non-transformed cells: embryonic rat cells,[8,10] primary chick embryonic cells,[4] neonatal rat cells (in this study) *etc*. The geodesic domes do not appear to be a mere culture artifact, given their ubiquitous occurrence in the epithelial layer of the lens in humans of all ages and many other species.[33] In the lens, three-dimensional shape changes take place to accommodate different focal lengths dynamically. This results in unique radial 3D patterns of tension, which might dictate the preferred existence of this particular CSK architecture. In stiffer lenses (such as in amphibians), which achieve accommodation *via* translation, rather than shape changes, geodome structures are rarely found.[33]

Cardiac fibroblasts represent a significant portion of the cell population in the heart. Recent reports reveal the essential mechanosensing ability of these cells.[34] Evidence for perturbed anisotropy and overall structural changes in load-related heart pathologies[35] might be linked to involvement of cardiac fibroblasts in these structural alterations and in the ensuing functional changes. Better understanding of the response of cardiac cells to microenvironmental cues can facilitate the development of more efficacious prevention and treatment options in hypertrophy and other load-related heart conditions.

Experimental

Primary cardiac fibroblast culture

Cardiac fibroblasts were cultured from neonatal rat hearts. Briefly, enzymatic digestion with trypsin and collagenase (Worthington Biochemical, Lakewood, NJ) was applied to the ventricles of 3-day old rats. Through a 45 min pre-plating procedure, fibroblasts (which attach first) were separated from cardiac myocytes. Four to six days later the fibroblasts were trypsinized (0.05% trypsin and 0.5 mM EDTA, Gibco, Grand Island, NY) and re-plated onto fibronectin-coated (50 μg ml^{-1}, BD Biosciences, Franklin Lakes, NJ) scaffolds at 20×10^3 cells per cm^2. The cells were maintained at 37 °C with 5% CO_2 in medium 199 (Gibco) supplemented with 2% fetal bovine serum (Gibco). All experiments were done with fibroblasts from first and second re-plating.

Scaffolds for the cell growth were prepared from polydimethylsiloxane or PDMS (Sylgard 184 from Dow Corning, Midland, MI) in the usual ratio of 1 : 10 of curing agent to elastomer and baked for 2 h at 60 °C. Additionally, standard glass and polyvinylchloride (PVC) coverslips (both from VWR, West Chester, PA) were used in some experiments. Each scaffold was cut to an approximate area of 1 cm^2. Topographic features of various sizes were introduced by molding PDMS from pre-manufactured micro-grooved masters using custom-developed non-photolithographic method, acoustic micromachining.[36] The resultant groove– peak guiding features with variable spacing were used to effectively produce anisotropy in the scaffolds, in the extracellular matrix and the cells grown on them.

Cytoskeleton-modulating agents

Cardiac fibroblasts were treated on day 2 of culture with 10 mM 2,3-butanedione 2-monoxime (BDM, Sigma, St. Louis, MO) for 24 h. Cytochalasin D (Sigma) was added to the fibroblast culture at 0.2 μM or 1 μM for 45 min to 3 h, previously reported to affect non-muscle cell CSK.[23]

Yeast treatment

Some previous studies have shown that *C. albicans* may secrete molecules that result in rearrangement of the actin CSK.[24,28] Therefore, to examine *local* perturbations of the cell actin network, we co-cultured the fibroblasts with *C. albicans* grown to form hyphae and attempted to correlate hyphae location with CSK structure. *C. albicans* with a mutation of the URA3 gene, CAI4 (*ura3*-), a gift from Dr J. B. Konopka (Stony Brook University), was first grown in yeast peptone broth, supplemented with uridine (5 mg ml^{-1}), YPDu. Cardiac fibroblasts were inoculated on day 2 of culture at high (2.5×10^5 ml^{-1}) or low (2.5×10^3 ml^{-1}) concentration. Control samples did not receive any treatment, while sham samples received YPDu, but no yeast. Cells were fixed 9 h after treatment. The mutant *C. albicans* used here did not reduce cell viability or cause contamination-related effects.

Fluorescent labeling

At days 2 to 7 after plating, the cells were fixed in 3.7% formaldehyde and permeabilized with 0.02% Triton-X 100. Cell CSK was stained with phalloidin–Alexa 488 (Molecular Probes, Eugene, OR) for F-actin. Nuclei were stained with TOTO-3 (Molecular Probes) for

confocal imaging or DAPI otherwise. Calcofluor White binds to cellulose and chitin in the cell wall of fungi and was used to label the yeast (Sigma, 0.5% (w/v)), under UV illumination.

Fluorescence imaging and data analysis

Samples were mounted on a glass slide with VectaShield (Vector Laboratories, Burlingame, CA). Fluorescence imaging was performed using a confocal laser-scanning microscope BioRad Radiance 2000 with a 60× oil-immersion objective (N.A. 1.4), or an inverted fluorescence microscope Nikon TS100 with a 40× objective (N.A. 0.95). In the latter case, images were taken with a microscope-attached Nikon Coolpix 995 digital camera. All images were properly scaled. For determining frequency of occurrence of the geodesic domes, five random fields per scaffold were imaged and analyzed. At least five scaffolds from different cultures were used per case. Geodesic domes were counted manually and related to the number of nuclei in the corresponding area. Data are presented at mean and standard error (mean ± s.e.m.). Statistical analysis was performed using a two-sided t-test.

Acknowledgments

We would like to thank Dr Konopka for the *Candida albicans* yeast strain, and students L. Yin, V. Dasari, M. Farrell and HJ Yu for help with image analysis. This study was partially funded by the Whitaker Foundation (RG-02-0654).

References

1. Lazarides E, Burridge K. Cell (Cambridge, MA, U S). 1975; 6:289–298.
2. Lazarides E. J Cell Biol. 1975; 65:549–561. [PubMed: 1094020]
3. Osborn M, Born T, Koitsch HJ, Weber K. Cell (Cambridge, MA, U S). 1978; 14:477–488.
4. Lin ZX, Holtzer S, Schultheiss T, Murray J, Masaki T, Fischman DA, Holtzer H. J Cell Biol. 1989; 108:2355–2367. [PubMed: 2472405]
5. Coughlin MF, Stamenovic D. Biophys J. 2003; 84:1328–1336. [PubMed: 12547813]
6. Discher DE, Boal DH, Boey SK. Biophys J. 1998; 75:1584–1597. [PubMed: 9726959]
7. Vera C, Skelton R, Bossens F, Sung LA. Ann Biomed Eng. 2005; 33:1387–1404. [PubMed: 16240087]
8. Badley RA, Woods A, Carruthers L, Rees DA. J Cell Sci. 1980; 43:379–390. [PubMed: 6774989]
9. Wang N, Tolic-Norrelykke IM, Chen JX, Mijailovich SM, Butler JP, Fredberg JJ, Stamenovic D. Am J Physiol. 2002; 282:C606–C616.
10. Lazarides E. J Cell Biol. 1976; 68:202–219. [PubMed: 1107334]
11. Lazarides E. J Histochem Cytochem. 1975; 23:507–528. [PubMed: 1095651]
12. Rathke PC, Osborn M, Weber K. Eur J Cell Biol. 1979; 19:40–48.
13. Ingber DE. J Cell Sci. 1993; 104(Pt 3):613–627. [PubMed: 8314865]
14. Clark P, Connolly P, Curtis AS, Dow JA, Wilkinson CD. Development (Cambridge, U K). 1990; 108:635–644.
15. Curtis ASG, Wilkinson CD. J Biomater Sci, Polym Ed. 1998; 9:1313–1329. [PubMed: 9860172]
16. Oakley C, Jaeger NA, Brunette DM. Exp Cell Res. 1997; 234:413–424. [PubMed: 9260912]
17. Mrksich M, Chen CS, Xia Y, Dike LE, Ingber DE, Whitesides GM. Proc Natl Acad Sci U S A. 1996; 93:10775–10778. [PubMed: 8855256]
18. Singhvi R, Kumar A, Lopez GP, Stephanopoulos GN, Wang DIC, Whitesides GM, Ingber DE. Science. 1994; 264:696–698. [PubMed: 8171320]
19. Bien H, Yin L, Entcheva E. IEEE Eng Med Biol Mag. 2003; 22:108–112. [PubMed: 14699943]

20. Yin L, Bien H, Entcheva E. Am J Physiol. 2004; 287:H1276–H1285.
21. Bischofs IB, Klein F, Lehnert D, Bastmeyer M, Schwarz US. Biophys J. 2008; 95:3488–3496. [PubMed: 18599642]
22. Huang S, Chen CS, Ingber DE. Mol Biol Cell. 1998; 9:3179–3193. [PubMed: 9802905]
23. Wakatsuki T, Schwab B, Thompson NC, Elson EL. J Cell Sci. 2001; 114:1025–1036. [PubMed: 11181185]
24. Marewicz E, Michalik M, Macura AB. Folia Histochem Cytobiol. 1995; 33:157–162. [PubMed: 8612867]
25. Collinsworth AM, Zhang S, Kraus WE, Truskey GA. Am J Physiol. 2002; 283:C1219–C1227.
26. Rotsch C, Radmacher M. Biophys J. 2000; 78:520–535. [PubMed: 10620315]
27. Peckham M, Miller G, Wells C, Zicha D, Dunn GA. J Cell Sci. 2001; 114:1367–1377. [PubMed: 11257002]
28. Tsarfaty I, Sandovsky-Losica H, Mittelman L, Berdicevsky I, Segal E. FEMS Microbiol Lett. 2000; 189:225–232. [PubMed: 10930743]
29. Wang N, Naruse K, Stamenovic D, Fredberg JJ, Mijailovich SM, Toric-Norrelykke IM, Polte T, Mannix R, Ingber DE. Proc Natl Acad Sci U S A. 2001; 98:7765–7770. [PubMed: 11438729]
30. Yarrow JC, Lechler T, Li R, Mitchison TJ. BMC Cell Biol. 2003; 4:5. [PubMed: 12783627]
31. Schliwa M. J Cell Biol. 1982; 92:79–91. [PubMed: 7199055]
32. Pourati J, Maniotis A, Spiegel D, Schaffer JL, Butler JP, Fredberg JJ, Ingber DE, Stamenovic D, Wang N. Am J Physiol. 1998; 274:C1283–C1289. [PubMed: 9612215]
33. Rafferty NS, Scholz DL. Curr Eye Res. 1989; 8:569–579. [PubMed: 2743796]
34. Ruwhof C, van Wamel AE, Egas JM, van der LA. Mol Cell Biochem. 2000; 208:89–98. [PubMed: 10939632]
35. Wolk R, Cobbe SM, Hicks MN, Kane KA. Pharmacol Ther. 1999; 84:207–231. [PubMed: 10596907]
36. Entcheva E, Bien H. Lab Chip. 2005; 5:179–183. [PubMed: 15672132]

Insight, innovation, integration

The cell cytoskeleton (CSK) is a key factor in transducing mechanical signals into biochemical signals and regulating cell function. Control of CSK architecture by microenvironmental cues provides means of affecting cell fate. Our study experimentally examines alternative forms of the cell actin cytoskeletal network in response to specific microenvironmental factors, *e.g.* structural anisotropy induced by microfabricated variable-topography scaffolds and CSK tension-regulating perturbations. Both of these were found to strongly influence the transition from the geodesic dome type of CSK, with ordered polygonal elements, to stress fibers. The ubiquitous occurrence of CSK geodesic domes in various cell types and species, including in humans, and their role as mediators in controlling cell function underlie the general interest in these CSK microarchitectures.

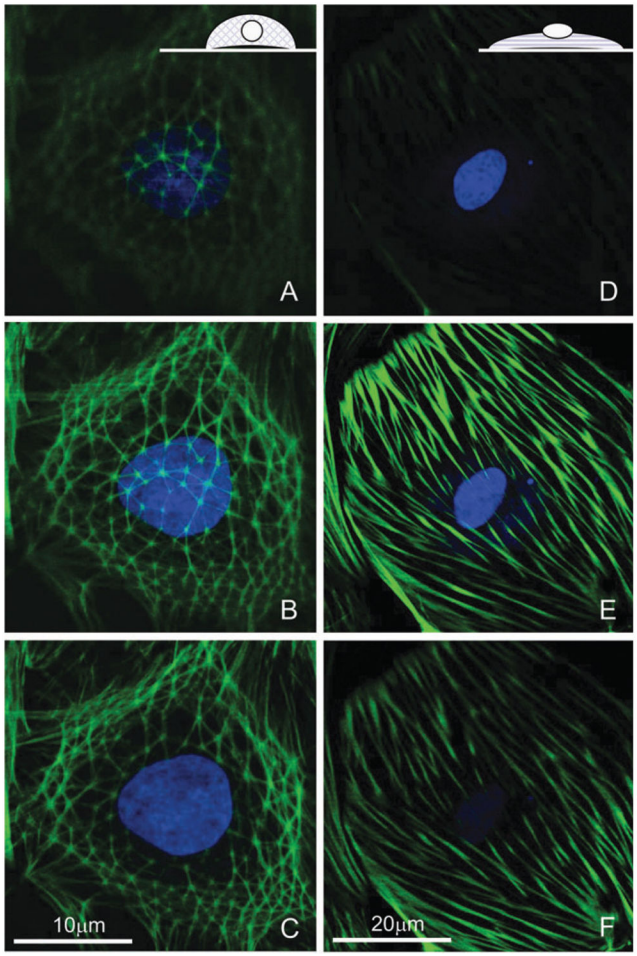

Fig. 1. Three-dimensional structure of the cytoskeleton in cultured cardiac fibroblasts

Geodesic domes (**A**–**C**) have a more apical appearance, extending higher above the scaffold surface, encompassing the nucleus, while typical stress fibers (**D**–**F**) run basally close to the surface, with the nucleus sitting on top. Inset cartoons in A and D illustrate the idea. Shown are confocal slices, 1 μm apart, of cells with labeled F-actin and nuclei (**C** and **F** are closest to the surface, **A** and **D** are furthest from the surface). Note the scale difference.

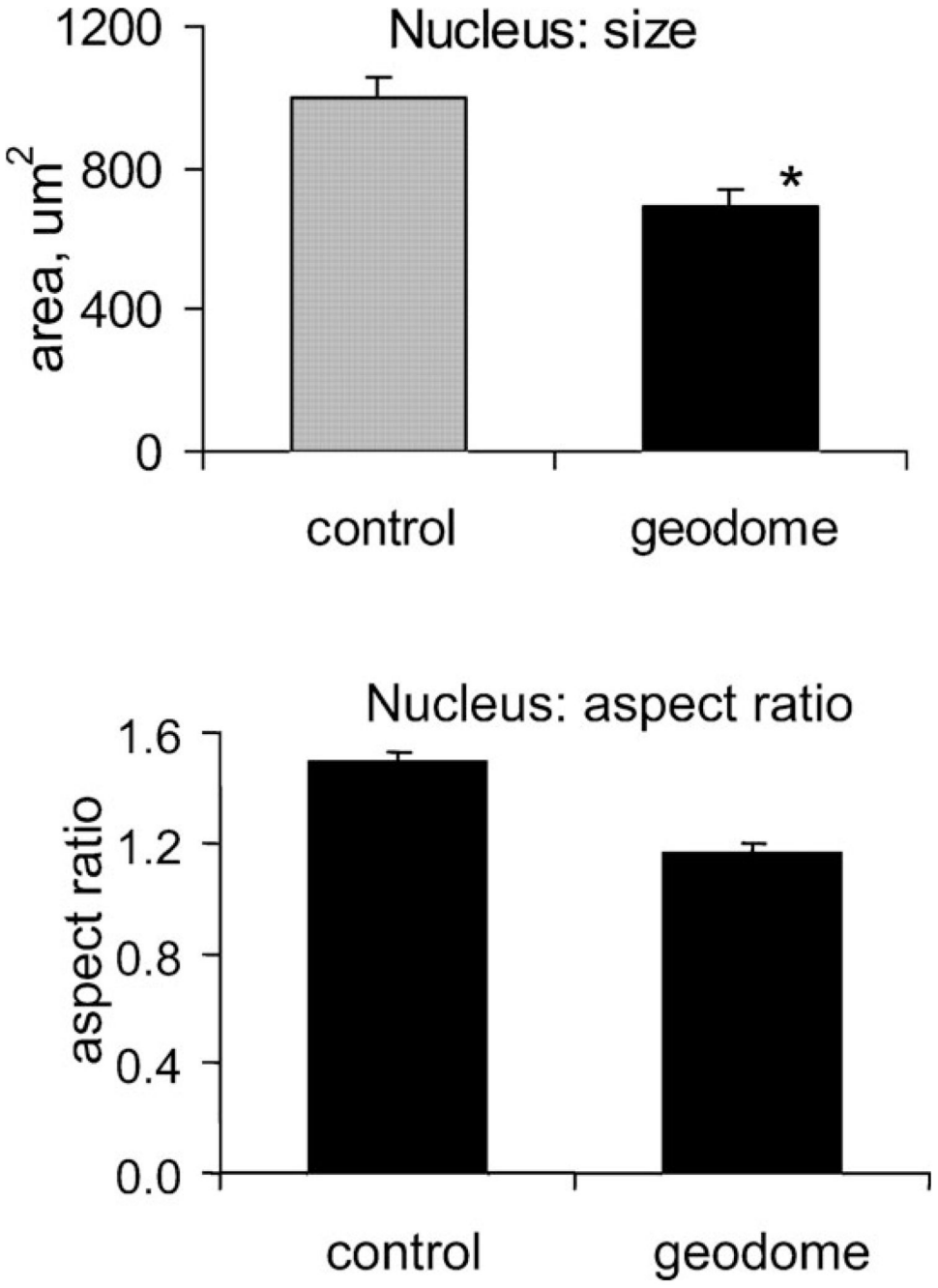

Fig. 2. Nuclear morphology in geodesic domes and control cells

Geodesic domes have nuclei that are smaller in size and closer to a perfect circle. Values are mean ± s.e.m. (*) indicates statistical significance at $p < 0.005$.

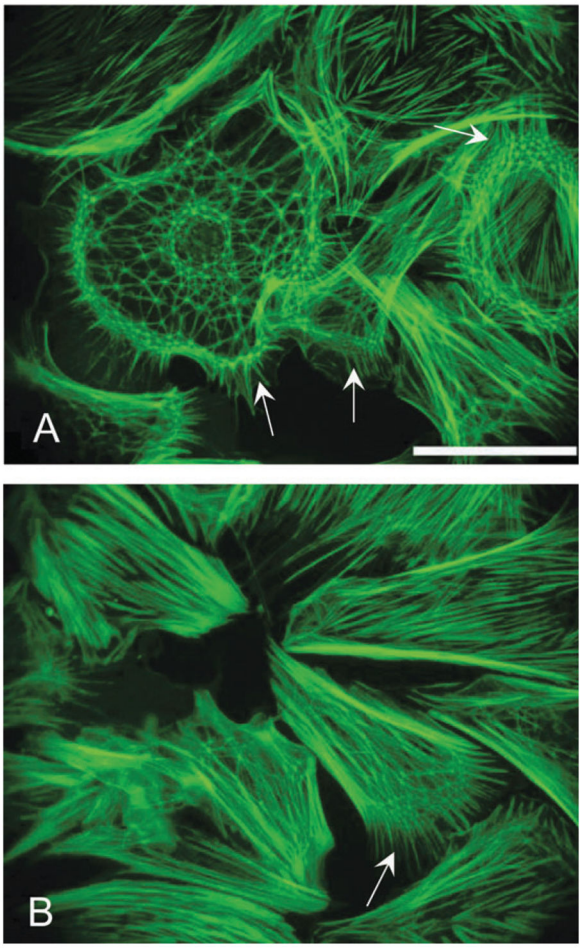

Fig. 3. Partial and whole polygonal nets

Whole geodesic domes (**A**) often exhibit higher net density in the cell periphery and the perinuclear actin regions. Partial polygonal nets typically are associated with the cells' periphery or the leading edge (arrows in **A** and **B**). Scale is 50 μm.

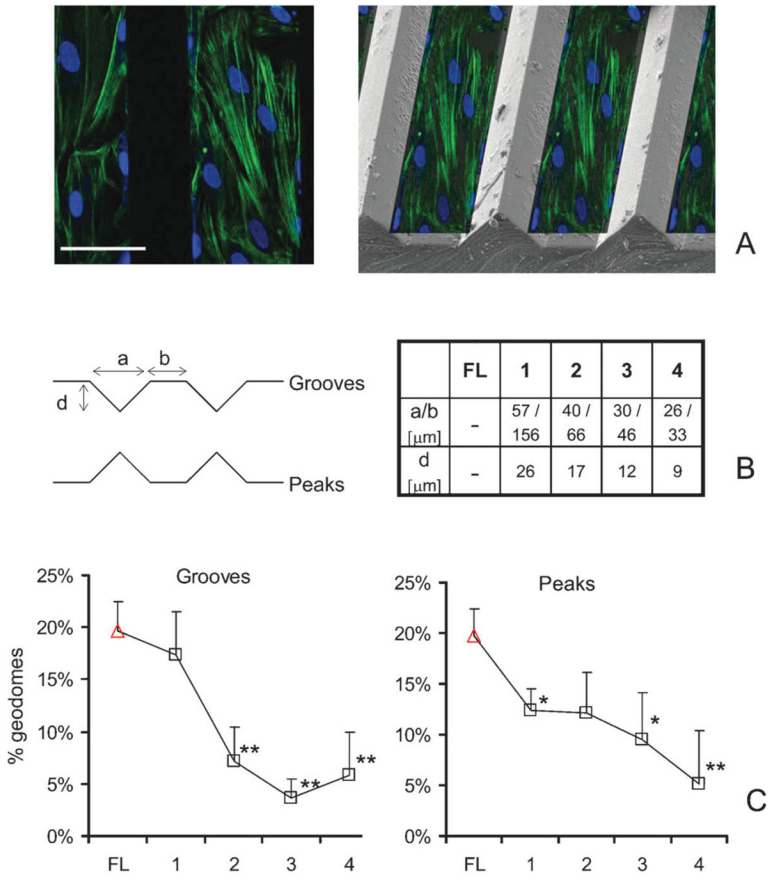

	FL	1	2	3	4
a/b [μm]	-	57 / 156	40 / 66	30 / 46	26 / 33
d [μm]	-	26	17	12	9

Fig. 4. Topographic control of geodesic domes

Scaffolds were designed with grooves and peaks of the specified dimensions to create 3D landscapes. (**A**-left) Confocal cross-section of cells grown on a Peak-2 surface and stained for F-actin and nuclei; (**A**-right) a collage of the fluorescently labeled cross-section overlaid on an actual scanning electron microscopy (SEM) image of a scaffold with a peak-type of surface, to illustrate relative position. (**B**) Schematic diagram of groove and peak types of surface with their corresponding dimensions. (**C**) More structured anisotropy-enforcing surfaces reduce the number of geodesic domes, when compared to flat (FL) surfaces. Values are mean ± s.e.m. (*) indicates statistical significance at $p < 0.05$, and (**) at $p < 0.01$. Scale is 50 μm.

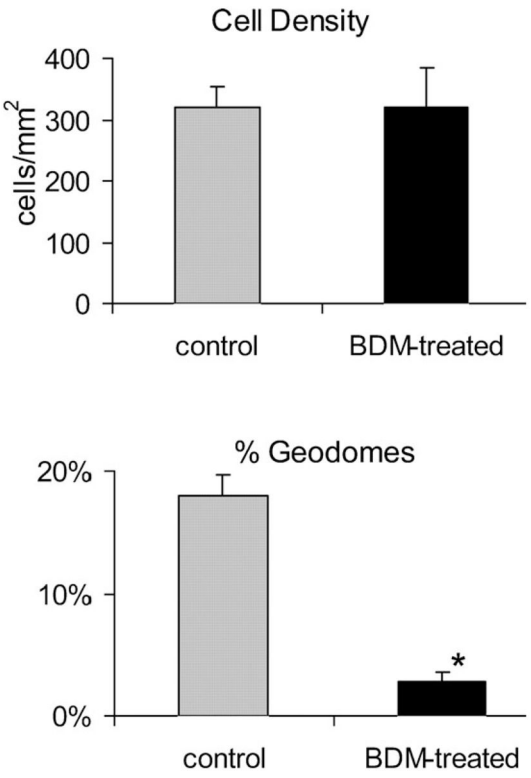

Fig. 5. BDM effects on the geodesic domes

Without an effect on cell density, BDM dramatically reduces the number of geodesic domes ($p < 0.00001$). Values are mean ± s.e.m.

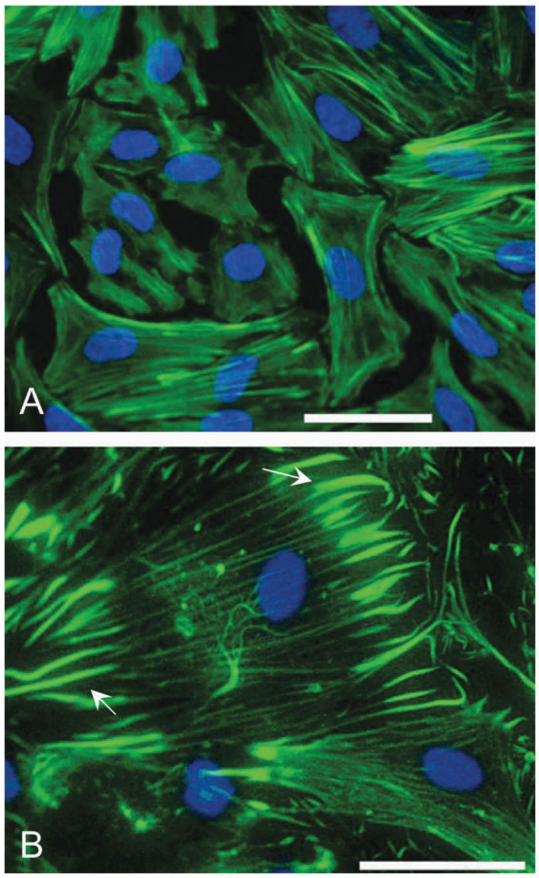

Fig. 6. Effects of BDM and cytochalasin D on the cytoskeleton

Actin perturbations in cardiac fibroblasts yield different results for BDM- (**A**) and cytochalasin D-treated cells (**B**). In BDM-treated fibroblasts the lamellipodium is altered—protrusions are eliminated. In cytochalasin D-treated cells the CSK is more dramatically disturbed—stress fibers disintegrate, with remnants visible at the focal adhesion sites (arrows). Geodesic domes are completely eliminated by cytochalasin D (1 mM for 3 h). Scales are 50 μm.

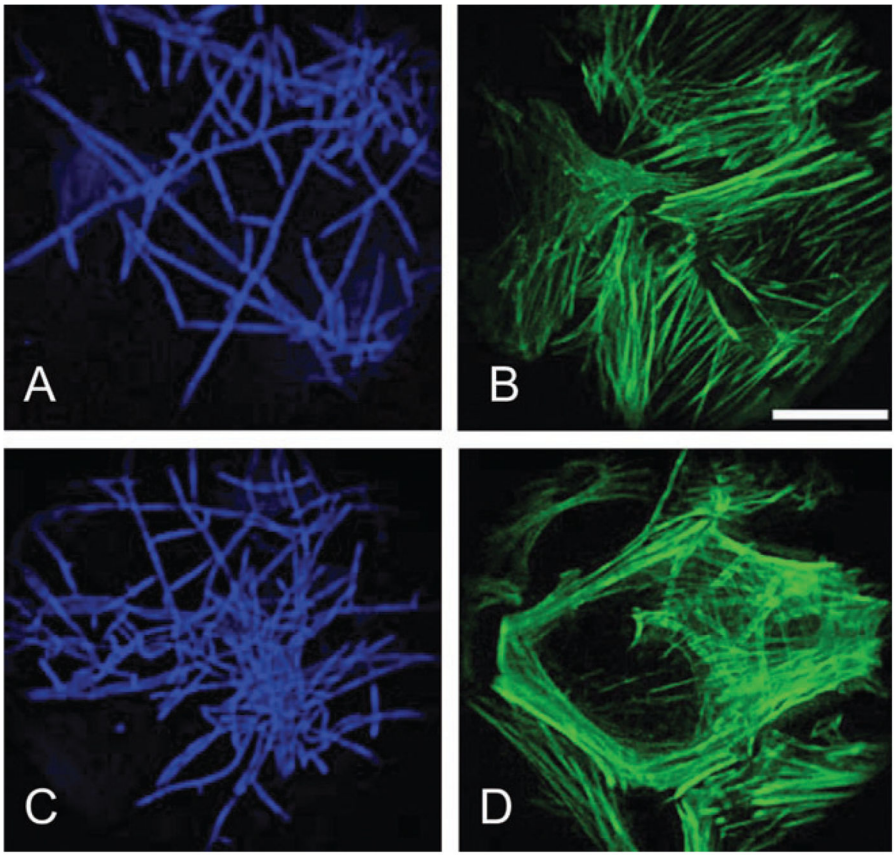

Fig. 7. Yeast (*Candida albicans*) effects on the cytoskeleton

Treatment with *C. albicans* for 9 h shows negligible (**B**) to significant (**D**) disturbance of the actin CSK underneath the fully developed hyphae (**A** and **C**). Cells are co-stained for yeast with Calcofluor white (**A** and **C**) and for F-actin with phalloidin (**B** and **D**). Scale is 50 μm.

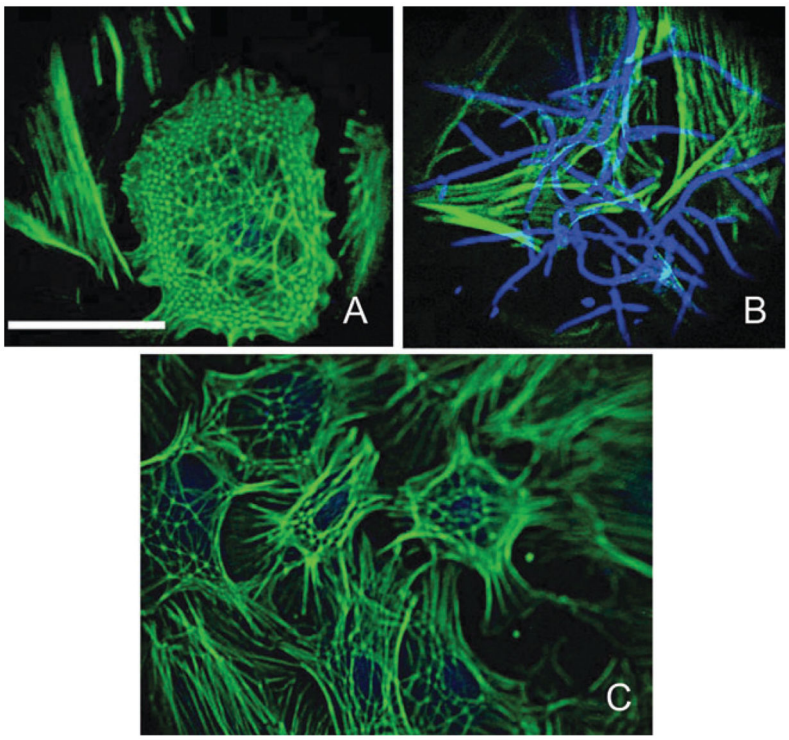

Fig. 8. Yeast and geodesic domes

The frequency of the geodesic domes is greatly reduced in the yeast-treated cells. More specifically, a local inverse relationship exists: no hyphae could be seen co-localized with the few remaining geodomes (**A** and **C**), and, conversely, no geodomes were present under the hyphae (**B**). Scale is 50 μm.